Chinese Chemical Letters 33 (2022) 3371–3383

Contents lists available at ScienceDirect

Chinese Chemical Letters

journal homepage: www.elsevier.com/locate/cclet

Advanced radionuclides in diagnosis and therapy for hepatocellular carcinoma

Hu Chen[1], Minglei Teng[1], Hongrui Zhang[1], Xiaoliu Liang, Hongwei Cheng*, Gang Liu*

State Key Laboratory of Molecular Vaccinology and Molecular Diagnostics, Center for Molecular Imaging and Translational Medicine, School of Public Health, Xiamen University, Xiamen 361005, China

ARTICLE INFO

Article history:
Received 3 February 2022
Revised 17 March 2022
Accepted 17 March 2022
Available online 21 March 2022

Keywords:
Radionuclide
Hepatocellular carcinoma
Diagnostic imaging
Endoradiotherapy
Precise medicine

ABSTRACT

Hepatocellular carcinoma (HCC) is the most common primary malignant tumor of the liver, but early diagnosis and effective treatment are still difficult. With the development of radionuclide applications in medicine, nuclear medicine is playing an increasingly important role in the diagnosis and treatment of HCC. Radionuclide-based positron emission tomography-computed tomography and single-photon emission computed tomography-computed tomography molecular imaging are indispensable for assessing progression, staging, differentiation, preoperative planning, postoperative prediction, and evaluation of HCC in clinical applications. Moreover, radionuclide-based endoradiotherapy provides an objective therapeutic strategy for patients with unresectable advanced HCC. This review highlights the application and development of radionuclides in the diagnosis and treatment of HCC. More efforts are warranted for the development of advanced radionuclides to make significant contributions in the treatment of HCC.

1. Introduction

Hepatocellular carcinoma (HCC) is the most common primary malignant tumor of the liver. It is often associated with cirrhosis, viral hepatitis (types B or C), and non-alcoholic fatty liver disease [1], and due to its high morbidity and mortality, it has a significant impact on human health and social development. Unlike many other tumor diseases, the diagnosis of HCC does not rely on tissue biopsy, and it can be diagnosed with imaging [2]. Enhanced computed tomography (CT) and magnetic resonance imaging (MRI) are widely accepted imaging methods for the diagnosis of HCC, but according to current diagnostic procedures, most patients are in the middle or late stages when they are diagnosed, and the treatment is often passive.

Although surgery and liver transplantation can cure HCC completely, they are only suitable for patients with early-stage HCC [3]. For patients with advanced HCC, chemotherapy, radiotherapy, and interventional therapy are usually used, but the overall therapeutic effect is not satisfactory [4]. With the continuous development of radiopharmaceuticals and equipment, new opportunities have been opened for the early diagnosis and treatment of cancer, including HCC. More and more studies have shown that nuclear medicine, molecular imaging, and targeted therapy are playing increasingly important roles in the diagnosis and treatment of HCC [5].

Over the past two decades, positron emission tomography (PET) and single-photon emission computed tomography (SPECT) imaging have been widely used in the diagnosis and evaluation of various cancers [6,7]. Especially since the advent of hybrid imaging techniques, such as PET/CT and SPECT/CT, molecular imaging has become more and more widely used for cancer diagnosis. With the expected growth of these imaging approaches, it has been recognized that new PET and SPECT probes are needed to address the clinical challenges of early diagnosis and staging of various types of cancer.

Radionuclide probes for HCC imaging are expanding and provide information on liver-metabolism function and the degree of tumor differentiation from multi-dimension perspectives for imaging monitoring of HCC [8]. 2-[^{18}F]fluorodeoxyglucose (^{18}F-FDG) is usually used as a tumor tracer, but beyond this, there is increasing evidence that radio-labeled choline tracers and other novel tracers may play an increasing role in liver tumor imaging [9]. PET/CT and SPECT/CT are now more active in the diagnosis of HCC and play an important role in clinical staging, preoperative analysis, metastasis diagnosis, and prognosis evaluation of HCC [6,7].

Surgical resection is usually the first choice in the treatment of HCC, but the resection rate is only 8%–25%. Hepatic transarterial chemoembolization (TACE) is the most commonly used method for

* Corresponding authors.
E-mail addresses: hongwei1026@hotmail.com (H. Cheng), gangliu.cmitm@xmu.edu.cn (G. Liu).
[1] These three authors contributed equally to this work.

https://doi.org/10.1016/j.cclet.2022.03.079
1001-8417/

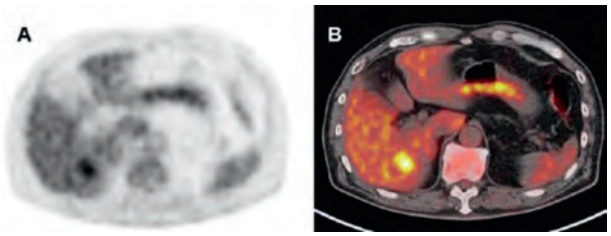

Fig. 1. ^{18}F-FDG PET image shows strong signal in normal liver (A). Fused PET/CT image clearly shows that the highest uptake in areas of tumor (B). Reproduced with permission [14]. Copyright 2015, Elsevier.

unresectable HCC [10]. Although this method has achieved remarkable clinical results, it can induce adverse effects on the whole body. Furthermore, about 30% of HCC patients are not sensitive to anticancer drugs, which limits the benefits of TACE to a certain extent.

In recent years, some combination therapies have been developed, including radionuclide-based radiotherapy [11]. Internal irradiation therapy with radionuclide can kill tumor cells in large quantities with few side effects and obvious efficacy, thus providing a promising treatment mode for unresectable HCC. With the continuous progress of therapeutic methods and vectors, internal irradiation has become one of the effective methods in the treatment of HCC [12]. At present, radionuclides used in the treatment of HCC in various forms include ^{131}I, ^{125}I, and ^{90}Y, among others. The strategy of radionuclide-based radiotherapy mainly includes transarterial radiation embolization (TARE), radioimmunotherapy (RIT), and endoradiotherapy.

2. Radionuclides in the diagnosis of HCC

2.1. ^{18}F

2.1.1. ^{18}F-FDG

^{18}F-FDG has a simple molecular structure, strong hydrophilicity, and is easy to obtain, thus representing the most successful tracer for PET. Currently, ^{18}F-FDG is the most commonly used positron tracer in clinical practice. The half-life of ^{18}F is relatively short at only 110 min. Rapid labeling and separation of ^{18}F imaging agent are necessary. Therefore, small integrated chemical synthesis modules have become a key step in the rapid preparation of PET radioimaging drugs.

At present, there are many chemical synthesis modules that can prepare ^{18}F-FDG. Each brand and model of chemical synthesis module follows the main process of ^{18}F-FDG production, but they differ slightly. There are two preparation principles for the chemical synthesis of ^{18}F isotope fluorination markers: electrophilic fluorination and nucleophilic fluorination [13]. Compared with electrophilic fluorination, the process chemistry of nucleophilic fluorination is simpler, and fluoride is more stable and convenient for separation and purification. Therefore, nucleophilic reaction with K2.2.2 is currently the most commonly used method.

In most cases, the diagnosis of HCC is based on CT or MRI findings, and biopsy is unnecessarily performed. These diagnostic methods result in a lack of information on the biological characteristics of the tumor. ^{18}F-FDG is commonly used as a radioactive tracer for tumor PET/CT imaging, and its uptake in HCC lesions has a definite correlation with tumor size and differentiation degree (Fig. 1) [14]. As for why ^{18}F-FDG can be used in imaging HCC, glucose transport protein (GLUT) plays a major role in the metabolism of ^{18}F-FDG in most malignant tumors. ^{18}F-FDG enters the cell and forms ^{18}F-FDG-6 phosphoric acid under the action of phosphohexokinase, which cannot further participate in aerobic or anaerobic metabolism. In general, ^{18}F-FDG-6 phosphoric acid cannot enter the cell membrane freely because of its negatively charge, which allows PET/CT imaging to show enhanced uptake of ^{18}F-FDG.

The higher uptake of radioactive tracer reflects the increased activity of glucose metabolism in cancer cells and the growth of malignant tissue, which is known as the Warburg effect. However, high FDG comorbidities in HCC demonstrate biological aggressiveness and associate with poor prognosis after treatment. ^{18}F-FDG PET/CT imaging has obvious advantages in the staging, re-staging, and pre-evaluation of HCC, but the positive detection rate of HCC is only 50%. Particularly, for the diagnosis of HCC with low differentiation, it is prone to false-negative results [15]. The role of FDG in imaging HCC may be negatively affected by the low level of expression of glucose-6-phosphatase and the high level of expression of glucose transporter-1 in HCC cells.

A large amount of glucos-6-phosphatase can dephosphorylate ^{18}F-FDG-6 phosphatase to generate free ^{18}F-FDG and release it from cells, resulting in a relatively low level of ^{18}F-FDG in tissues. It is also associated with low GLUT-1 and GLUT-2 levels or high p-glycoprotein expression. In addition, high uptake of ^{18}F-FDG in normal liver tissues is associated with high rates of gluconeogenesis, which may reduce the tumor-to-normal ratio (TNR) of tumors and the detection rate of HCC. Due to the reduced retention of parietal cells in tumors, detection of HCC is further restricted by the physiological limitations of the increased background of FDG uptake, which can be seen in some normal liver parenchyma [16].

Although PET scanning is not recommended for the detection of HCC due to FDG's low sensitivity, PET/CT with FDG provides more information about routine liver imaging [6]. PET/CT with ^{18}F-FDG may further improve the accuracy of diagnosis, staging, recurrence, and evaluation of biological characteristics of hepatic malignant tumors by diagnostic algorithms. Thus, they can benefit patients with primary lesions or metastatic liver tumors [17].

FDG-based PET imaging allows for the simultaneous assessment of perfusion status and metabolic activity. One retrospective study collected 5-min dynamic PET/CT and conventional PET/CT scans of 17 patients with pathologically diagnosed HCC using a dual-input dual-compartment uptake model. The results showed that perfusion and early uptake of PET/CT increased the positivity rate of HCC, and additional functional information could be provided to improve the diagnostic level [18]. Simultaneous PET/MRI systems and ^{18}F-FDG were used to evaluate the relationship between metabolism and water diffusion rate of liver tumors, as well as to reveal the metabolic and diffusion characteristics of different types of liver tumors. The results showed that the maximum standard uptake value (SUVmax) was negatively correlated with apparent diffusion coefficient (ADC), and each group of tumors had different metabolic and water-diffusion characteristics [19].

A retrospective study shown that ^{18}F-FDG-based PET/CT has some value in the diagnosis of intrahepatic tumors before and after treatment. When recurrent or extrahepatic metastasis occurs, normal multistage CT can be recognized. The size improvement shown by anatomical imaging may be insensitive to early stage, while metabolic imaging may detect tumor recurrence. FDG is highly sensitive to the detection of HCC extrahepatic metastasis and recurrent tumors. In a systematic review and meta-analysis, Lin *et al.* found that PET/CT with ^{18}F-FDG was helpful in ruling out extrahepatic metastasis of HCC and could also be used to rule out recurrent HCC [20].

The accurate characterization of liver damage by ^{18}F-FDG has limited value, but it has been shown to have an important impact on the prognosis of HCC patients. Cho *et al.* evaluated ^{18}F-FDG as an independent prognostic factor in 104 patients with newly diagnosed HCC [21]. They found that a high ratio of SUVmax to the mediastinal mean SUV was significantly associated with the tumor load index, AFP value, aminotransferase level, tumor size, and the

Barcelona Clinic Liver Cancer (BCLC) stage. A meta-analysis of 22 studies showed that both a high tumor SUVmax ratio and a high tumor SUVmax value for normal liver are associated with poor prognosis in HCC patients [22]. Regarding prognosis after treatment, a multi-center retrospective study showed that tumor uptake of FDG was an independent prognostic factor for overall survival (OS) [23]. In addition, ^{18}F-FDG-based PET before treatment has certain value for risk assessment and prognosis prediction of surgical resection of HCC, HCC transplantation, and radioactive embolization [24].

The prognostic value of FDG uptake in HCC has been shown to be associated with specific gene expression. It has been proven that there is a strong correlation between the incorporation degree of FDG and pathological grade. Most interestingly, tumors with high glycolysis activity show stronger biological attack characteristics, and their gene expression is closely related to cell survival, intercellular adhesion, and cell diffusion [25]. The addition of FDG to the confirmation of HCC can be reasonably considered as a radiographic biomarker of bio-invasiveness. Studies on their relationship with the expression of programmed death ligand 1 (PD-L1) and angiogenesis in large cohort studies have shown that high SUVmax in ^{18}F-FDG PET/CT is associated with poorer clinical outcomes and PD-L1 expression in HCC patients [26].

2.1.2. ^{18}F-Fluorocholine

Choline is a precursor of phospholipid synthesis and is involved in the biosynthesis of phosphatidylcholine and cell membranes. As a precursor of phospholipids, choline is an essential component of cell membrane synthesis. Tumor cells proliferate rapidly, which increases the activity of cell membrane biosynthesis, choline kinase activity, and choline intake. After entering a tumor cell and being phosphorylated, choline cannot cross the cell membrane. Instead, it remains in the cell, maintaining a "chemical stasis". This is the rationale for cholinergic imaging of tumors. In clinical application, choline-based PET/CT can greatly make up for the deficiency of ^{18}F-FDG-based PET/CT in some tumor applications and improve the accuracy of tumor diagnosis.

In addition, choline-based PET/CT can distinguish HCC from focal nodular hyperplasia, and choline intake is significantly higher in HCC than in nodular hyperplasia. It has been proposed that the use of dual-imaging agents (2-[^{18}F]fluorocholine (^{18}F-FCH) and ^{18}F-FDG) in PET/CT can be more effective in diagnosing HCC, with diagnostic efficiency increasing from 63% to 89% [27]. A series of comparative studies indicate that although the physiological uptake of choline in the liver is high, the activity choline kinase in relation to choline metabolism in HCC tissues is significantly higher than that in surrounding normal tissues, and HCC nodules can still be detected visually [28–30].

The tumor recurrence rate of HCC patients is more than 50% within 5 years after surgery. Using reduced ^{18}F-FCH metabolism as a criterion for judging malignancies improves the detection rate for HCC and has similar value to ^{18}F-FDG in predicting early recurrence after resection of single-focal HCC [31]. Systematic reviews and meta-analyses suggest that radio-labeled choline PET/CT is a valuable tool for the detection of moderately differentiated HCC compared to FDG PET/CT [6]. Thus, choline PET/CT has high diagnostic value for medium to well-differentiated HCC, while FDG PET/CT has high diagnostic value for poorly differentiated hepatocellular carcinoma and liver metastasis.

2.1.3. Novel ^{18}F-labeled imaging agent

To fully use the advantages of ^{18}F in imaging and improve the diagnostic efficiency of HCC, researchers have developed and explored many novel ^{18}F-labeled probes. Horsager *et al.* studied PET with the liver-specific galactose tracer 2-[^{18}F]fluoro-2-deoxy-D-galactose (^{18}F-FDGal) [32]. It was found that whole-body images acquired after ^{18}F-FDGal injection do not offer an advantage over traditional whole-body PET/CT images for detection of HCC. Recently, Li *et al.* prepared a novel ^{18}F-labeled imaging agent, [^{18}F]AIF-NOTA-G-TMTP1, by a NOTA-AIF chelation method for PET for the diagnosis of highly metastatic HCC [33]. It is well known that TMTP1 has a high affinity for a range of highly metastatic tumor cells. NOTA is coupled to TMTP1 by a glycine residue, which provides a spacer function to maintain its own activity and improve its excretory dynamics. The results showed that [^{18}F]AIF-NOTA-G-TMTP1 can specifically target HCC with high metastasis, displaying the low background activity. Thus, it has potential for use as an imaging agent to detect tumor lesions in the liver region.

2.2. ^{64}Cu

The prospect of using ^{64}Cu in the simple Cu^{2+} ion form as a PET probe is not only a cost-effective proposition, but also seems promising to broaden the palette of molecular imaging probes for the foreseeable future. The use of the $^{64}Cu^{2+}$ ion as a PET probe is based on the fact that Cu is an essential element that plays an important role in cell proliferation and angiogenesis. In recent years, evidence has been constantly emerging from animal models of $^{64}Cu^{2+}$ uptake in HCC, colorectal cancer, prostate cancer, lung cancer, and other types of tumors [34]. Copper metabolism in human HCC was assessed using PET with copper(II)-64 chloride ($^{64}CuCl_2$) as a tracer. The expression of human copper transporter 1 (hCTR1) in HCC cells and tissues was detected by real-time reverse transcription polymerase chain reaction and immunohistochemistry. The results showed that $^{64}CuCl_2$ PET imaging can locate human HCC tumors that were transplanted in mice, which provides the possibility of locating and quantitatively evaluating copper metabolism in metastatic HCC tumors in humans [35].

A series of novel probes based on ^{64}Cu were also explored for HCC. Li *et al.* developed a PET tracer to monitor CD38 expression in HCC using the anti-CD38 monoclonal antibody (daratumumab). In this study, daratumumab was radiolabeled with ^{64}Cu to obtain ^{64}Cu-Nota-daratumumab. CD38 is expressed on the surface of many immune cells and is closely related to the anti-tumor immunity and immune tolerance of tumor cells. Cell studies and PET imaging have demonstrated the CD38 imaging capability and specificity of [^{64}Cu]Cu-NOTA-daratumumab in HCC mouse models. [^{64}Cu]Cu-NOTA-daratumumab is an effective PET tracer that can be used to noninvasively evaluate CD38 expression and sensitively detect CD38-positive tumor lesions in HCC [36].

2.3. ^{89}Zr

^{89}Zr is a positron radionuclide that the half-life is 78.4 h and it has a relatively low positron energy (395.5 keV). ^{89}Zr is relatively safe to be operated and has low production cost for PET imaging. Therefore, it has a certain application potential in molecular imaging diagnosis. The membrane protein glypican-3 (GPC3) is overexpressed in 50% of HCC patients and is associated with early HCC, so it can be served as a potential molecular target for early HCC detection. For example, ^{89}Zr-coupled monoclonal antibody against GPC3 ([^{89}Zr]Zr-αGPC3) was used for PET imaging of intrahepatic tumors. The results indicated that [^{89}Zr]Zr-αGPC3 exhibited antigen-specific and antigen-dependent tumor binding, confirming the feasibility of imaging diagnosis for HCC and qualitative detection of GPC3 expression by ^{89}Zr-αGPC3 in small animals [37]. Similarly, ^{89}Zr-coupled F(ab')2 fragment to target GPC3 ([^{89}Zr]Zr-αGPC3-F(ab')2) was also used to validate the feasibility as a diagnostic immune-PET imaging probe. However, the sensitivity and specificity of [^{89}Zr]Zr-αGPC3-F(ab')2 probes need to be further optimized during clinical translation [38]. In addition, anti-GPC3 monoclonal antibody (clone 1G12) conjugated with ^{89}Zr can be

used for specific and high contrast imaging for GPC3 positive HCC, which may contribute to early detection of HCC and timely intervention [39]. In a follow-up study, the team humanized mouse antibodies using complementary determination region (CDR) grafting to produce a cloned H3K3 antibody that retains the same binding affinity and specificity as human GPC3 for diagnostic imaging in patients with HCC [40]. In another study, GPC3-targeted antibody αGPC3 was conjugated to ^{89}Zr and ^{90}Y, respectively, to evaluate the therapeutic response in a mouse HCC model. As expected, the GPC3-targeted ^{89}Zr and ^{90}Y therapeutic platform could effectively evaluate the response to RIT in a GPC3-expressing HCC xenograft model [41].

Overexpression of CD146 is associated with aggressiveness, recurrence rates, and poor overall survival in patients with HCC. Cai's team developed a CD146 targeting probe for high-contrast, non-invasive PET and near-infrared fluorescence (NIRF) imaging of HCC. The anti-CD146 monoclonal antibody YY146 was used as the target molecule, coupled with NIRF dye ZW800–1 and DF. This allows DF-YY146-ZW800 to be labeled with ^{89}Zr for PET and NIRF imaging without affecting antibody binding properties. The results showed that [^{89}Zr]Zr-DF-YY146-ZW800 possessed good properties as PET/NIRF imaging agent, including high affinity and specificity for CD146-expressing HCC *in vivo* with great potential for early detection, prognosis and image-guided surgical resection of liver malignancies [42].

2.4. ^{124}I, ^{68}Ga and ^{11}C

^{124}I has a long half-life (4.15 d) and excellent nuclear characteristics ($\beta+$: 25.6%, electron capture (EC): 74.4%). Compared to other conventional positron radionuclides, ^{124}I can provide higher-quality PET/CT images for disease diagnosis. Carrasquillo *et al.* explored the application value of [^{124}I]I-codrituzumab in PET imaging of HCC. Codrituzumab (also known as GC33) is an antibody against glypican 3. This study shows that quantitative imaging using ^{124}I-antibodies is technically feasible and that they can be used successfully to image a number of HCC patients [43].

^{68}Ga is a PET radionuclide that can be obtained from a long-life ^{68}Ge/^{68}Ga generator without reliance on accelerators. $T_{1/2}$ of ^{68}Ga is shorter (68.3 min), and it could be used as an imaging probe to effectively reduce the radiation dose for patients. One study has compared the performance of ^{68}GA-labeled fibroblast activating protein inhibitor (FAPI) PET and ^{18}F-FDG PET in liver tumor imaging. Compared with ^{18}F-FDG, [^{68}Ga]Ga-FAPI PET/CT was reported to have greater potential in the detection of primary liver malignant tumors [44]. It is believed that ^{68}Ga-PSMA PET/CT may also play a role in the diagnostic imaging of HCC. PSMA is known for its relation to prostate cancer and is overexpressed in prostate epithelial cells, but it has been shown to be highly expressed in the tumor blood vessels and membrane of HCC [45]. A small prospective study found that [^{68}Ga]Ga-PSMA PET/CT was superior to FDG PET/CT in HCC patients [46].

[C_1–^{11}C]acetate (^{11}C-ACT) is a lipid tracer. Acetate is a precursor of fatty acids for conversion to acetyl-CoA, and overexpression of fatty acid synthase in tumor cells may increase acetate accumulation of acetate as a marker of tumor activity. Many studies have confirmed that [C_1–^{11}C]choline PET/CT has a higher detection rate than FDG PET/CT. Choline PET/CT has a higher detection rate for moderately highly differentiated HCC and a lower detection rate for poorly differentiated HCC [47]. It has been suggested that [C_1–^{11}C]-methionine may be a useful choice for detecting extrahepatic lesions and could provide additional information on suspected cases if they metastasized far away. The application value of ^{11}C-ACT in HCC has been confirmed, but due to the short half-life of ^{11}C, it can only be produced in PET/CT centers equipped with cyclotrons and the number of cases that can be examined at a time is limited in clinical practice.

2.5. ^{99m}Tc

Among medical radionuclides, ^{99m}Tc is the best single photon radionuclide ($t_{1/2} = 6.01$ h, $E\gamma = 140$ keV). It can be readily obtained from a ^{99}Mo-^{99m}Tc generator, and ^{99m}Tc-radiopharmaceuticals can be easily prepared by labeling precursors of their cartridge (KIT). In addition, technetium has various valence states ranging from -1 to $+7$, and its rich coordination chemical properties provide broad prospects for application in the design and synthesis of technetium radioactive drugs with different biological distribution characteristics.

^{90}Y microsphere radioembolization (RE) is a promising catheter treatment option for patients with unresectable primary and metastatic liver tumors. Its theoretical basis comes from the double blood supply of liver tissue through the hepatic artery and portal vein. Angiographic evaluation is typically performed prior to treatment in combination with [^{99m}Tc]Tc-macroaggregated albumin (^{99m}Tc-MAA) scans to map the blood vessels supplying the tumor and to avoid accidental deposition of microspheres in organs other than the liver.

SPECT/CT can be directly associated with anatomical and functional information in patients with unresectable liver disease. Pre-treatment SPECT/CT is an important component of the treatment plan, including catheter location and dose discovery. Bremsstrahlung (BS) scan after treatment should follow RE to verify the distribution of the given tracer. BS SPECT/CT imaging allows better localization and determination of intrahepatic and possibly extrahepatic spherical distribution, as well as some degree of post-treatment dosimetry (Fig. 2) [7]. In the pre-treatment evaluation of ^{90}Y-radiation embolization, ^{99m}Tc-MAA SPECT/CT has been found to reflect the biological distribution of liver particles more accurately than hepatic angiography with soluble contrast agent. Thus, it should be a key criterion in the selection of patients with ^{90}Y-radiation embolization. ^{99m}Tc-MAA SPECT/CT provides more information than planar scintillation imaging to guide radiotherapy and prognostic evaluation [48].

SPECT/CT has a significant influence on the location of the catheter tip and hepatic tumor load during drug administration. In current clinical practice, the ^{99m}Tc-MAA distribution does not accurately predict the final ^{90}Y activity distribution. Awareness of the importance of catheter positioning and adherence to specific recommendations may lead to the optimization of individualized treatment plans based on preprocessing imaging [49]. One study compared ^{99m}Tc-MAA SPECT uptake before treatment with ^{90}Y-bremsstrahlung SPECT uptake after treatment. The results revealed that ^{99m}Tc-MAA SPECT has certain prognostic value for radiation embolism with ^{90}Y-labeled resin microspheres [50].

However, it was found no correlation between the imaging time of ^{99m}Tc-MAA and the uptake of extrahepatic radiotracer, and the value of evaluating *in vivo* distribution was questioned [51]. Haste *et al.* confirmed that ^{99m}Tc-MAA is a poor quantitative predictor of hepatocellular carcinoma as a substitute for activity distribution of ^{90}Y [52]. For proper planning of the embolization activity of ^{90}Y in the liver, toxicity and efficacy should be balanced. Recently, Lam *et al.* developed a dual-tracer SPECT fusion imaging protocol that combines radiometric distribution data with physiological liver mapping. This technique provides a physiology-based imaging tool with significant prognostic power that may lead to improved personalized activity planning [53].

Various ^{99m}Tc-labeled probes have also emerged in the imaging diagnosis of liver cancer. The liver uptake value (LUV) can be calculated reliably using SPECT/CT fusion images obtained with ^{99m}Tc-labeled galactose-human serum albumin ([^{99m}Tc]Tc-GSA), and the

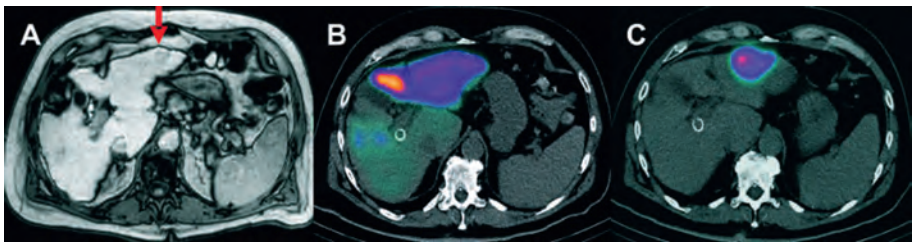

Fig. 2. (A) Patient with HCC in whom RE of a single HCC in the left liver lobe (MRI scan, red arrow) was planned with the ^{99m}Tc-MAA SPECT/CT. (B) The first test angiogram shows diffuse tracer accumulation in the left liver lobe and no specific uptake in the tumor area. (C) The second test angiogram after placing the catheter tip more distally shows accentuated accumulation in the tumor area without any relevant uptake in the noninvolved liver. Reproduced with permission [7]. Copyright 2014, Springer.

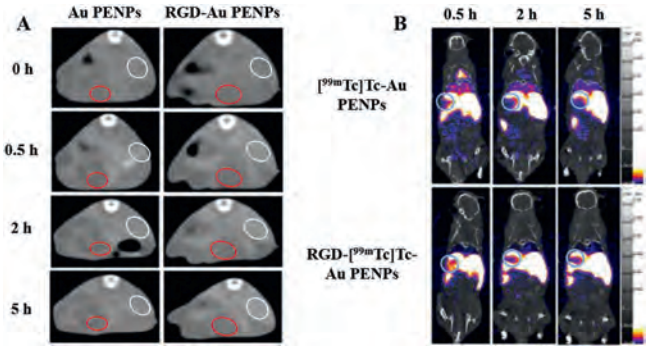

Fig. 3. (A) *In vivo* CT images of the RGD−Au PENPs or non-targeted Au PENPs in an orthotopic hepatic carcinoma model *via* intravenous administration at different time points post-injection (red circle refers to the hepatic carcinoma region, white circle refers to normal liver region). (B) *In vivo* SPECT/CT images of the RGD-[^{99m}Tc]Tc-Au PENPs or [^{99m}Tc]Tc-Au PENPs in HCC (noted as green circle) after intravenous administration at different time points post-injection Reproduced with permission [57]. Copyright 2018, American Chemical Society.

result can be used to assess liver function [54,55]. A recent study showed that [^{99m}Tc]Tc-GSA SPECT image-guided reverse planning (IGIP) has a dose advantage over conventional planning in preserving liver function. Kai *et al.* reported the first clinical use of [^{99m}Tc]Tc-GSA SPECT IGIP in stereotactic body radiotherapy (SBRT) for HCC. As expected, they achieved a complete response using the target volume assessment. ^{99m}Tc-GSA SPECT-IGIP SBRT re-irradiation can successfully and safely save recurrent HCC [56].

The specificity and stability of probes are very important in the diagnosis of HCC. Zhou *et al.* reported on ^{99m}Tc-labeled arginine-glycine-aspartic acid (RGD)-polyvinyl imine (PEI) conjugates with entrapped gold nanoparticles (RGD-[^{99m}Tc]Tc-Au PENPs) as a dual-mode SPECT/CT imaging probe for HCC (Fig. 3). The results showed that the designed RGD-[^{99m}Tc]Tc-Au PENPs had good colloid stability, radio-stability, and biocompatibility in the experimental concentration range. Furthermore, they could be specifically absorbed by hepatocellular carcinoma cells overexpressing $\alpha_v\beta_3$ integrin *in vitro*. *In vivo* SPECT/CT imaging results showed the aggregated particles *in situ* in HCC and enhanced CT and SPECT in tumor tissue [57].

2.6. ^{131}I

With a half-life of 8.02 d, ^{131}I emits a small amount of γ rays during β decay, making it suitable for precise medical imaging. Hao *et al.* reported that [^{131}I]I-anti-AT1R monoclonal antibody (mAb) could be an effective imaging reporter for the detection of HCC. Angiotensin type II 1 receptor (AT1R) has been reported to be elevated in a variety of tumors and to be involved in tumor progression. Whole-body autoradiography, the biological distribution, and pharmacokinetics of [^{131}I]I-anti-AT1R were studied by injecting HCC mice *via* the tail vein [58]. In another study, [^{131}I]I-anti-TLR5 mAb was used as a novel radiotracer for imaging hepatoma in H22 tumor mice. Toll-like receptor 5 (TLR5) is overexpressed in several cancers and metastases and is an attractive target for molecular imaging of primary tumors. The results showed that [^{131}I]I-anti-TLR5 mAb can be used to detect lesions expressing TLR5 tumors with highly targeted selectivity. Thus, it may provide a promising drug for the diagnosis of HCC and encourages further research [59].

2.7. Induction and summary

The application value of radionuclides introduced above is different according to their own characteristics and applicable probes, and they all have their own advantages and disadvantages. In order to conveniently realize the application of each radionuclide in the imaging diagnosis of HCC, the main application value and characteristics are listed in Table 1.

3. Radionuclides in therapies for HCC

Radionuclides have been clinically applied in the treatment of HCC for over 20 years, and the most widely used are ^{131}I and ^{90}Y, which emit β rays with low linear energy transfer (LET) [60]. ^{131}I is easy to prepare, cheap, and applicable in gamma ray imaging. It also has a physical half-life of 8 d and a simple protein chemical labeling method, so it is widely used. Compared with external irradiation with X-rays, internal irradiation based on radionuclides has an advantage of doing less damage to normal liver tissue. The treatment of liver cancer by internal irradiation mainly includes embolization radiotherapy by interventional means, intratumoral puncture particle implantation, and antibody-targeted radioimmunotherapy.

Radioimmunotherapy involves the use of antibodies labeled with radionuclides to target a tumor area, stay within it, and eliminate the tumor through the effects of both antibodies and radionuclide irradiation. The main function of antibodies is to infiltrate the tumor tissue and be taken up by it to achieve selective aggregation of radionuclides in the tumor. In recent years, a variety of small molecular antibody structures with lower molecular weight than full-antibody IgG have been used for RIT. They can easily penetrate into tumor tissues and bind to tumor antigens. Therefore, a higher radioactivity ratio (T/NT) of tumor to non-tumor tissues can be obtained [61]. However, they have low antigenicity and can be quickly cleared by normal tissues. At present, only F(ab')2 fragments and Fab' single fragments have shown good tumor targeting and clinical efficacy [62].

Hepatic tumors are mainly supplied by the hepatic artery, while normal liver is mainly supplied by the portal vein. Therefore, intra-arterial treatments, including TACE and TARE, are considered palliative care. With the development of nuclear and radiochemical techniques, TARE has become an alternative option for patients with HCC, especially in cases where other therapies have failed or

Table 1
Major radionuclides used for imaging diagnosis of HCC.

Radionuclide	Half-life	Imaging probe	Application	Comment/Properties
^{18}F [a]	109.77 min	^{18}F-FDG	Definite differentiation degree [14]; assess perfusion status and metabolic activity [18]; evaluate the relationship between metabolism and water diffusion rate [19]; detect HCC extrahepatic metastasis and recurrent tumors [20]; prognostic prediction [21–24]	Low cost and convenient imaging; false-negative for HCC with low differentiation; high background of FDG uptake
		[^{18}F]fluorocholine	Diagnose and distinguish HCC from focal nodular hyperplasia [27–30]; detect moderately differentiated HCC [6]; predict early recurrence [31]	High accuracy of tumor diagnosis and high diagnostic value for medium to well-differentiated HCC
		[^{18}F]FAlf-NOTA-G-TMTP1	Diagnose highly metastatic HCC [33]	Specifically target HCC with high metastasis and display the low background activity
^{64}Cu [a]	12.701 h	[^{64}Cu]$CuCl_2$	Locate and quantitatively evaluate copper metabolism in metastatic HCC [35]	Simple and easy to obtain, but high systemic distribution
		[^{64}Cu]Cu-Nota-daratumumab	Evaluate CD38 expression and sensitively detect CD38-positive tumor lesions [36]	Lack of clinical studies
^{89}Zr [a]	78.41 h	[^{89}Zr]Zr-αGPC3	Imaging diagnosis for HCC and qualitative detection of GPC3 expression [37]; evaluate the response to RIT [41]	Relatively safe to be operated and has low production cost; antigen-specific and antigen-dependent tumor binding
		[^{89}Zr]Zr-αGPC3-F(ab')2	Localization of intrahepatic tumors [44]	Sensitivity and specificity need to be further optimized
		[^{89}Zr]Zr-DFO-1G12	Early detection of HCC [39]	Specific and high contrast imaging for GPC3 positive HCC
		[^{89}Zr]Zr-DF-H3K3	Diagnostic imaging [40]	Humanized mouse antibodies retains the same binding affinity and specificity as human GPC3
		[^{89}Zr]Zr-DF-YY146-ZW800	Early detection, prognosis and image-guided surgical resection of liver malignancies [42]	High affinity and specificity for CD146-expressing HCC; multimodal imaging performance
^{124}I [a]	4.1760 d	[^{124}I]I-GC33	Quantitative imaging [43]	Provide higher-quality PET/CT images
^{68}Ga [a]	67.71 min	[^{68}Ga]Ga-FAPI	Detect primary liver malignant tumors [38]	Effectively reduce the radiation dose
		[^{68}Ga]Ga-	diagnostic imaging [46]	May superior to ^{18}F-FDG
^{11}C [a] Higher detection rate for moderately highly differentiated HCC	20.364 min	[C_1–^{11}C]ACT	Evaluate tumor activity	Higher detection rate than FDG PET/CT
		[C_1–^{11}C]choline	Diagnostic imaging [47]	
		[C_1–^{11}C]methionine	Detecting extrahepatic lesions	
^{99m}Tc [b]	6.0067 h	[^{99m}Tc]Tc-MAA	Map the blood vessels and guide radiotherapy [48,53]; verify the distribution of ^{90}Y [52]; evaluate post-treatment dosimetry [7]	Easily prepared; convenience and direct information feedback; less accidental deposition
		[^{99m}Tc]-GSA	Assess liver function [54,55]	Successfully and safely save recurrent HCC
		RGD-[^{99m}Tc]Tc-Au PENPs	Diagnostic imaging [57]	Specifically absorbed by HCC cells overexpressing $\alpha v\beta_3$ integrin
^{131}I [b]	8.0252 d	[^{131}I]I-anti-AT1R mAb	Diagnostic imaging [58]	Detect lesions AT1R-expressing tumors selectivity
		[^{131}I]I-anti-TLR5 mAb	Diagnostic imaging [59]	Detect lesions expressing TLR5 tumors with highly targeted selectivity

[a] Imaging type: PET.
[b] Imaging type: SPECT.

those requiring down-staging therapy. In practice, some radionuclides have the appropriate physicochemical properties to serve as radioactive embolization agents [63].

Radioactive particle implantation methods, such as ^{125}I-seed implantation (ISI), are another type of treatment for HCC. Particle implantation techniques include inter-tissue implantation, portal vein implantation, inferior vena cava implantation, and biliary duct implantation. These are used to treat intrahepatic lesions, portal vein cancer thrombus, inferior vena cava cancer thrombus, and intrabile duct cancer or cancer thrombus, respectively. Compared with ordinary external irradiation, radioactive particle implantation has advantages of higher local doses to the tumor and less systemic radiation damage.

Relative biological effectiveness (RBE) and lower toxicity may be more advantageous than β particles in tumor therapy, α particles can be used for systemic targeted radiotherapy for primary and metastatic tumors, especially for hematological tumors and small tumor ranges widely distributed throughout the body [64]. In combination with the metabolic pathway, half-life and availability of α radionuclides *in vivo*, the main radionuclides studied in clinical and preclinical studies are ^{225}Ac, ^{227}Th, ^{213}Bi, ^{211}At, ^{212}Pb and ^{223}Ra [65]. In recent years, targeted alpha-particle therapy (TAT)

has attracted more attention in clinic with the rapid development of small molecule ligands, peptides, antibodies and nanomaterials targeting ligands and vectors.

3.1. ^{90}Y

^{90}Y emits only β rays with a range of nearly 12 mm and higher energy (2.28 MeV), making it more suitable for radiotherapy for larger tumors. It also has fewer restrictions in regard to environmental radiation safety, but it has a strong affinity with bone, so bone marrow can be damaged by high doses of radiation. In addition, because γ photons are not emitted, *in vitro* scintillation imaging cannot be used to detect the distribution of ^{90}Y *in vivo*. Therefore, angiography and ^{99m}Tc-MAA scanning are required before treatment to calculate the percentage of gastrointestinal and pulmonary shunt in injection activity to avoid toxic reactions. Generally, shunt over 13% is not suitable for treatment [66].

^{90}Y-RE is a treatment where ^{90}Y spheres are delivered *via* the arteries to the liver. The principle of ^{90}Y-RE involves the selective delivery of a high amount of radiation to the liver tumor and a low dose to the surrounding normal parenchyma. ^{90}Y-RE can be thought of as a combination of embolization and radiation therapy, so standard radiological follow-up models may not be sufficient to assess the tumor response to therapy accurately.

^{90}Y-microspheres come in two types: resin and glass. Since glass microspheres have higher activity per particle, they can deliver a specific radiation dose with fewer particles, likely reducing the embolization effect. Therefore, glass microspheres may be more suitable for early stasis or regurgitation in the context of HCC with portal vein invasion and radiation segmentectomy. Due to the low activity per particle of resin microspheres, more particles are required to provide a specific radiation dose. Therefore, resin microspheres may be more suitable for tumors that are larger or have high arterial flow.

Precise treatment plans can lead to more effective and safer treatment by delivering a higher radiation dose to the tumor while minimizing exposure to the surrounding liver parenchyma. The treatment plan relies largely on the estimated radiation dose to the tissue. Quantitative imaging (^{90}Y SPECT/CT or ^{90}Y PET/CT) after microsphere treatment can be used to calculate the macroscopic absorbed dose distributions *in vivo* [67]. Taebi *et al.* used computational fluid dynamics (CFD) simulations in a three-dimensional hepatic artery tree model to illustrate the uneven distribution of microspheres between segments of the liver [68]. The results demonstrated the importance of developing patient-specific dosimetry methods for effective radioembolization.

However, this treatment always results in a degree of irradiation to the normal liver parenchyma, inducing a different radiological appearance. Unlike other interventional treatments, it can take months for a tumor response to become apparent when using TARE. In addition, during follow-up, there are many imaging findings related to the surgery itself, which make image interpretation and efficacy evaluation difficult [69]. The use of nuclear medicine imaging can provide valuable information for predicting the tumor response to TARE. PET/CT has recently proven to be a viable alternative to post-infusion imaging, providing high-quality images of ^{90}Y-loaded microspheres after selective internal radiation therapy (SIRT). Patient-specific dosimetry is also possible as long as accurate absolute PET calibration is performed and the collection time is long enough. The threshold dose of objective response to HCC was prospectively assessed using paired PET with ^{90}Y to quantify the dose of radiation to hepatic tumors after embolization. The dose of embolization was calculated from PET images, and the image segmentation was performed by volume analysis of the dose deposition in tumors [70]. Although Monte Carlo calculations appear to be superior to all dose estimation algorithms, the data from D'Arienzo *et al.* provide a strong argument in favor of the use of local deposition algorithms in routine ^{90}Y dosimetry based on PET/CT imaging because of its simplicity of implementation [71].

There is increasing information about the dose-response and dose-toxicity associations in the liver of TARE, but few studies have investigated dose-toxicity associations in extrahepatic tissues. A patient-specific dosimetry method based on the Monte Carlo technique has been described for the study of lung injury after TARE [72]. It was found that radiation-induced focal lung injury occurred at a significantly higher absorbed dose than the cumulative lung dose given in a single dose or during TARE. Another study has shown that the lung fractional rate (LSF) may be significantly overestimated when using planar imaging and can be more accurately calculated using SPECT/CT imaging and appropriate segmentation tools [73]. Minimizing errors in obtaining LSF could lead to more effective SIRT treatment plans for HCC with ^{90}Y microspheres selective internal radiotherapy, while ensuring that the lung dose does not exceed the standard acceptable threshold for safety.

The feasibility of ^{90}Y-RE in the treatment of HCC has been demonstrated [74]. ^{90}Y microspheres are also used in the treatment of liver metastasis of cancer, liver metastasis of rectal cancer, and liver metastasis of patients with neuroendocrine tumors [75]. In addition, the safety and efficacy of ^{90}Y glass microspheres have been evaluated in the treatment of unresectable localized metastatic liver disease [76]. Anatomical variations may potentially increase the risk of non-target vessel embolization during ^{90}Y radioembolization due to the close proximity of the hepatic and intestinal vessel branches. The safety of ^{90}Y-RE with resin microspheres in patients with different anatomical structures of the hepatic artery also needs to be considered. Zimmermann *et al.* reported that ^{90}Y-RE is safe in an abnormal hepatic artery at a safe distance of least 1.9 cm from the tip of the microcatheter [77]. For the non-invasive imaging diagnosis, rapid-airway-stimulation blood oxygen level-dependent MRI was used to evaluate the changes of tumor hypoxia after ^{90}Y-RE in a VX2 rabbit model [78]. According to other studies, ^{90}Y-RE combined with drug eluting beads preloaded with irinotecan (DEBIRI) show good anti-tumor activity in the treatment of a VX2 rabbit model [79].

3.2. ^{166}Ho

The European Union has recently approved [^{166}Ho]Ho-poly(lactic acid) (PLLA) microspheres for clinical use in patients with HCC. The isotope ^{166}Ho is attractive because it emits high-energy radiation that can be used for therapeutic effects without gamma camera saturation and gamma rays that can be used for SPECT/CT imaging. In addition, due to the paramagnetic and high density properties, ^{166}Ho can be observed by MRI and CT. Currently, some ^{166}HO-labeled compounds are used in patients, such as ^{166}Ho-labeled microspheres for radioembolization of HCC [80]. The ^{166}Ho microspheres can be used as both a reconnaissance dose (250 MBq) and a therapeutic dose. The general toxicity and safety of accidental extrahepatic deposition of ^{166}Ho-scout dose (^{166}Ho-SD) were studied by Arthur *et al.*, and the safety of 250 MBq ^{166}Ho-SD was demonstrated in clinical use [81]. Notably, MRI can directly observe holmium deposition after administration and may be adapted to treatment if necessary. Roosen *et al.* explored ^{166}Ho microspheres for SIRT under being visualized and quantified by MRI, making it possible to conduct MRI guidance during SIRT [82].

In vivo dose monitoring, similar to ^{90}Y embolization, the dose estimation and distribution can also be performed with ^{99m}Tc before and after embolization of ^{166}Ho. As an alternative to ^{99m}Tc-MAA, ^{166}Ho microspheres with reconnaissance dose can be used

before embolization of ^{166}Ho for predicting intrahepatic distribution. The application of the same particles in the pretreatment and the treatment program can improve the predictive value of the pretreatment distribution analysis. Smits *et al.* analyzed the consistency between ^{166}Ho-scout and ^{166}Ho-therapeutic dose, and compared the consistency between ^{99m}TC-MAA and ^{166}Ho-therapeutic dose [83]. It was found that ^{166}Ho-scout has a higher predictive value for intrahepatic distribution of ^{166}Ho microspheres than ^{99m}TC-MAA. The accuracy of ^{99m}Tc-MAA based lung absorbed dose estimation was compared with ^{166}Ho microsphere imaging based on pre-diagnosis and the actual lung absorbed dose after embolization of ^{166}Ho by Elschot *et al.* [84]. It was demonstrated that ^{99m}Tc-MAA imaging obviously overestimates the absorbed lung dose in clinical application and pre-diagnosed ^{166}Ho microsphere SPECT/CT imaging can accurately predict the lung absorbed dose after embolization [85]. However, compared to ^{99m}Tc-MAA, accidental extrahepatic deposition of this β-emitting scout dose can cause radiation damage. In response to this concern, Prince *et al.* quantified the extent of radiation damage of ^{166}Ho microspheres. Retrospective studies have shown that extrahepatic deposition of ^{166}Ho at a scout dose is theoretically safe in most patients and its safety was being evaluated in clinical trials [86]. For therapeutic radioembolism, highly active ^{166}Ho microspheres are used, which is ideally for dosimetry with direct subsequent SPECT imaging. Stella *et al.* evaluated gamma camera performance and SPECT image quality with high ^{166}Ho activity and proved the feasibility of this strategy [87]. Additionally, in order to accurately predict the biological distribution of ^{166}Ho microspheres with ^{99m}Tc, Rooij *et al.* proposed a dual-isotope SPECT protocol based on ^{166}Ho microspheres and ^{99m}Tc stannous phytate, and showed that this novel ^{166}Ho/^{99m}Tc dual isotope protocol for automated dosimetry can accurately compensate for downward scattering, allowing the addition of ^{99m}Tc without compromising ^{166}Ho SPECT image quality [88].

In a phase 1 dose escalation study, safe and efficacy of ^{166}Ho microspheres were certified for radioembolization of liver metastases that were not suitable for surgical resection [89]. Results showed that ^{166}Ho microsphere radioembolization induced tumor response without significant toxicity in salvage patients. Bastiaannet *et al.* then investigated the relationship between absorbed dose and response and their association with overall survival of ^{166}Ho radioembolization in patients with liver metastasis [90]. The results confirmed that tumor response is closely rely on absorbed dose of ^{166}Ho and was simultaneously associated with a higher overall survival.

Other types of microspheres based on ^{166}Ho are also being explored. A novel microdevice that polylactic acid (PLLA) microspheres loaded with [^{166}Ho]Ho-acetyl acetone ([^{166}Ho]Ho-PLLA-MS) was prepared *via* the solvent evaporation technique [91]. In this study, the synthetic microspheres possessed characteristics with uniform size and surface morphology, complex stability, radiochemical purity and resistibility to neutron irradiation, providing good evidence for their potential application in radioembolization. Furthermore, in order to reduce the treatment cost of TARE, Subramanian *et al.* prepared ^{166}HO labeled Biorex^{TM} 70 microsphere that had pleasing yield, splendid stability, and good retention, indicating that the application of these indigenous radiolabeled microspheres in the treatment of HCC has potential and deserves further study [92].

3.3. ^{131}I

^{131}I is one of the radionuclides that are widely used in clinical RIT and has a physical half-life of 192 h, a maximum β-ray energy of 0.61 MeV, an average energy of 0.18 MeV, a maximum range of 2.30 mm, and an average range of 0.39 mm in soft tissue. To achieve intrahepatic radiotherapy of ^{131}I, it is necessary to have appropriate vectors for directional aggregation and retention in the liver, as well as to achieve an ideal match between the half-life of ^{131}I and the maximum local concentration of the vector in the tumor [93]. Importantly, it is required that the carrier itself does not cause a severe allergic reaction, and its binding with ^{131}I should be stable, have little shedding in the body, and have a high binding rate.

At present, mainly two kinds of vectors are commonly used [94]. One is biological agents (mainly monoclonal antibodies of hybridoma), which have opened up a new field for specific passive immunotherapy, but ideal clinical effect equivalent to that of immunomodulators has not been achieved. The second type is embolic materials, such as [^{131}I]lipiodol (^{131}I-LUF) and [^{177}Lu]Lu-LUF (^{177}Lu-LUF), which have suitable particle size for embolization of middle and small arteries of HCC. In addition, lipiodol has the advantage of selectively accumulating in HCC tissues, which enables ^{131}I-labeled lipiodol emulsions to be absorbed by tumor tissues to the maximum extent, and there is very little impact on tissues and organs other than the liver. Therefore, patients have good tumor reactivity and tolerance. Transarterial injection of ^{131}I-LUF emulsion is suitable for multiple HCC foci or local treatments such as radiofrequency ablation, as well as for the treatment of subclinical HCC. The feasibility of ^{131}I-LUF TARE therapy has been proven by experiments and clinical practice. Moreover, an advantage of this method is that the vasculature of the liver can be preserved without affecting or limiting the selection indications for liver transplantation.

Schwarz *et al.* treated 38 patients with ^{131}I-LUF at a dose of 2220 MBq for 4 months post-operatively, and the results showed that it can improve the disease-free survival rate of HCC patients [95]. A systematic review and meta-analysis by Ruelan *et al.* also showed that adjuvant ^{131}I-LUF extends disease-free survival. It was found that liver function was preserved in most patients, and microvascular invasion was generally low [96]. Although the trend towards adjuvant therapy is worth highlighting, this treatment does not significantly improve overall survival. The prolongation of disease-free survival after ^{131}I-LUF adjuvant therapy provides a basis for further research on adjuvant intra-arterial therapy to improve the overall survival of HCC patients. Efforts should be made to establish guidelines on the timing and radiation dose of ^{131}I-LUF administration in order to normalize the potential use of this unique and evidence-based adjuvant therapy for HCC.

New embolization agents labeled with ^{131}I have also been widely explored in liver cancer embolization. Chi *et al.* prepared ^{131}I-gelatin microspheres (^{131}I-GMSS) with the chloramine T method and studied their effects on human hepatoma cells (HepG2) in nude mice (Balb/C), as well as their biological distribution after intratumoral injection. The results showed that ^{131}I-GMSS inhibited the growth of HepG2 and remained in tumors for a long time after injection [97].

In other work, a highly tumor-specific ^{131}I-TARE agent with long retention was developed by simply introducing tyrosine into polyvinyl alcohol (PVA) drug-eluting microspheres (Tyr-PVA-DEBs) (Fig. 4). Micro-SPECT/CT showed that ^{131}I-labeled microbeads accumulated for 31 d after intra-arterial injection of N1S1 HCC in rats. In addition, ^{131}I-labeled microbeads were loaded with doxorubicin hydrochloride (DOX) *via* a carboxyl group on the polymer tyrosine. The results showed that the ^{131}I-labeled embolization agent has a high tumor retention rate and a synergistic therapeutic effect on the treatment of liver cancer by low-dose trans-arterial chemoradiotherapy embolization (TARCE), indicating potential for clinical application [98]. However, the non-biodegradability and rapid deposition of microsphere materials lead to unsatisfactory distribution and preclude multiple drug administration.

Pang *et al.* prepared biodegradable chitosan collagen complex microspheres (CCMs) with an ideal sedimentation rate. The results

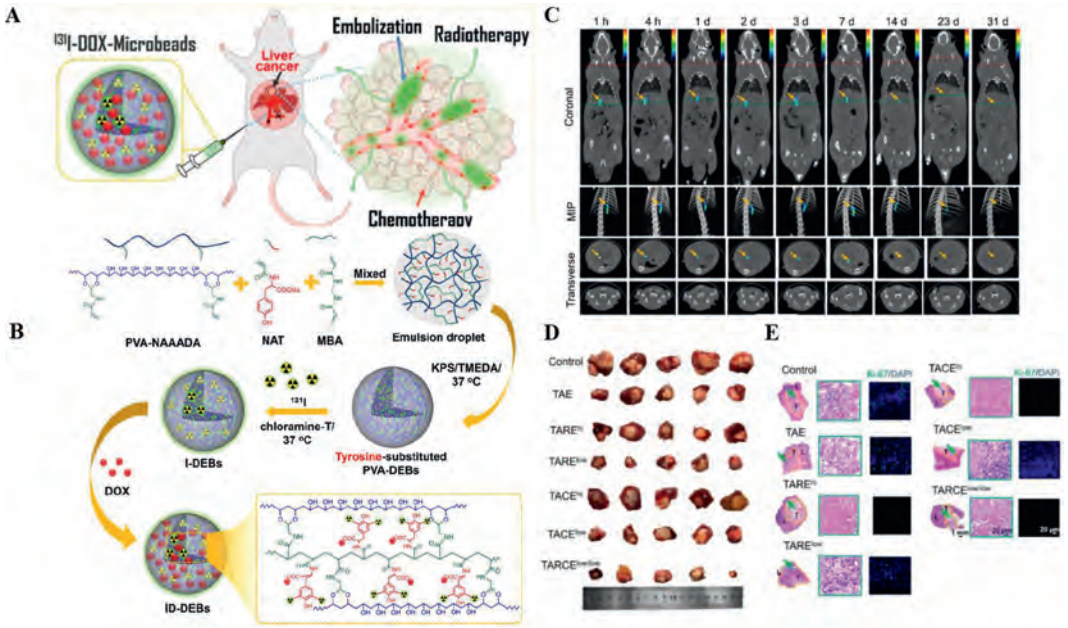

Fig. 4. Highly tumor-specific and long-acting ^{131}I-DOX microbeads for enhanced treatment of HCC with low-dose radio-chemoembolization. (A) Schematic diagram of treatment strategy. (B) Schematic illustration of ^{131}I-DOX-loaded drug-eluting microbeads (ID-DEBs). (C) TAE of ID-DEBs was detected with SPECT/CT. (D) Photographs of the resected tumors, (E) micrographs of H&E staining and Ki-67 immunofluorescence of each group at 14 d following the treatment. Reproduced with permission [98]. Copyright 2021, American Chemical Society.

showed that CCMs had the best radiolabeling efficiency, stability, and a good radioembolization effect in a mouse model of HCC. Thus, CCMs could have potential in interventional cancer therapy [99]. ^{131}I is an ideal radionuclide for RIT because of its convenient availability, easy labeling, appropriate half-life, moderate energy, short range of radiation release, and good marker stability. When ^{131}I decays, the β rays released by ^{131}I not only can kill tumor cells directly within range, but also expand the killing range of tumor cells through "cross interaction" between ^{131}I atoms that emit β rays.

HAbl8G/CD147 antigen expressed on cell surfaces is a highly glycosylated transmembrane protein composed of 269 amino acids and is one of the antigens associated with HCC, which plays an important role *in-situ* invasion and distant metastasis of HCC. [^{131}I]I-metuximab (^{131}I-mab) is a newly developed drug that targets CD147 and has been proven to be effective in clinical RIT for primary HCC [100]. In an earlier study, a combination of ^{131}I and CD147 monoclonal antibody was used to treat HCC in a rabbit VX2 animal model [101]. The findings suggested that [^{131}I]I-CD147-mab is a promising drug for the treatment of HCC, reducing the expression of matrix metalloproteinase 2 (MMP2) and CD31 or inducing tumor necrosis by inhibiting metastasis and growth. Afterwards, ^{131}I-mab and CD147-mab could significantly inhibit the growth of transplanted tumor, and ^{131}I-mab was more effective than CD147-mab [102]. The results of this study elucidated the mechanism of anti-proliferation and anti-metastasis effects of ^{131}I-mab and provided a theoretical basis for the clinical application of ^{131}I-mab. About 90% of the blood supply of HCC comes from the hepatic artery, so direct injection of antibodies through this artery can maximize the binding rate of antibodies and antigens [103]. Therefore, ^{131}I-mab is often used in clinical combination with TACE. Based on the targeting effect of tumor-specific antibodies, ^{131}I-mab exhibits a double killing effect of monoclonal antibodies and radiation to deliver a precise "cross strike" to target cells and avoid damage to other organs in the body [104]. Based on this concept, ^{131}I-mab was administered by hepatic artery infusion in clinical trials, which helped to improve HCC control in some patients [105].

Studies have confirmed that HAb18G/CD147 antigen is closely related to tumor recurrence and can be used as an independent risk factor for predicting recurrence after HCC resection or liver transplantation [106]. Bian *et al.* [107] reported that patients with CD147-positive HCC who received ^{131}I-mab were also shown to have a better response. In addition, Xu *et al.* [108] conducted a prospective study to evaluate the effect of ^{131}I-mab in preventing postoperative recurrence of HCC in patients after liver transplantation. The results showed that the one-year recurrence rate of patients treated with ^{131}I-mab was 26.7%, which was significantly lower than that of the placebo group at 57.1%.

A meta-analysis showed that TACE combined with ^{131}I-mab infusion in the treatment of unresectable HCC improved local efficacy and OS [109]. Similarly, ^{131}I-mab combined with TACE was found to prolong the survival time of HCC patients compared with TACE alone, and the combination therapy was safe and effective [110]. To further confirm the therapeutic benefits of ^{131}I-mab, some scholars believe that follow-up studies should ideally be conducted on a global scale and include a larger proportion of non-HBV-infected HCC patients [111].

With the development of nanotechnology, nano-drugs have greatly improved the treatment and diagnosis of liver cancer [112]. Taking the advantages of nanomedicine, ^{131}I-labeled nanoparticles provide a new therapeutic strategy for the diagnosis and treatment of HCC. Liver cancer stem cells (LCSCs) are thought to be associated with occurrence, development, metastasis, and recurrence of HCC. Thus, a novel strategy for targeting LCSCs was designed and studied using ferroplatinum nanoparticles (Fept-NPs) as a carrier and CD133 antigen as a target, which were combined with the HSV-TK suicide gene, ^{131}I radionuclide irradiation, and magnetic fluid hyperthermia (MFH) [113]. With PEI-FePt-NPs as a vector, LCSCs were transfected with pHRE-Egr1-HSV-TK and had a good transfection effect. ^{131}I-anti-CD133McAb was successfully prepared with 100% radiochemical purity and labeling rate of 36%, showing good radio-stability. PEI-FePt-NP-mediated gene therapy combined with magnetic fluid hyperthermia (pHRE-Egr1-HSV-TK/[^{131}I]I-anti-CD133McAb/MFH) can effectively inhibit LCSC proliferation and in-

duce cell apoptosis. This study provides a theoretically sound and feasible method for the treatment of LCSC, but has been limited to *in vitro* experiments.

Lin *et al*. studied the *in vitro* and *in vivo* targeting effect of [^{131}I]I-anti-AFPMcAb-GCV-BSA-NPs on AFP-positive HCC. Compared with ^{131}I alone, [^{131}I]I-anti-AFPMcAb-GCV-BSA-NPs are more easily absorbed and retained by HCC tissues and have a higher T/NT ratio. [^{131}I]I-anti-AFPMcAb-GCV-BSA-NPs have good drug loading, a high encapsulation rate, and high selective affinity for AFP positive tumors, so they are expected to be effective in gene therapy for HCC radiotherapy [114]. Similarly, Ji *et al*. designed and prepared a combination of radiotherapy and chemotherapy for albumin nanospheres, [^{131}I]I-anti-AFPMcAb-DOX-BSA-NPs. The results showed that [^{131}I]I-anti-AFPMcAb-DOX-BSA-NPs could significantly inhibit the growth of hepatocellular carcinoma [115]. Thus, nanomedicine based on ^{131}I-radiotherapy could provide new ideas for efficient therapeutic strategies for HCC.

3.4. ^{125}I

^{125}I is a radionuclide with a long half-life ($t_{1/2} = 59.7$ d). It releases low-energy γ rays (27 keV, characteristic X-ray) without β radiation, so it is widely used in the clinical diagnosis of nuclear medicine, biomedical research, and brachytherapy for tumors. Especially in recent years, the clinical application of ^{125}I radioactive seeds has been developed rapidly, its efficacy has been affirmed, and it is recognized as a safe and effective for treatment low complication rates. Brachytherapy with ^{125}I is currently one of the effective and safe treatment options for HCC complicated by portal vein tumor thrombosis (PVTT) [116,117].

A meta-analysis suggested that ^{125}I-irradiated stents are more effective in the treatment of HCC with portal vein tumor thrombosis. Portal vein stenting combined with intravascular brachytherapy may be an alternative therapy for PVTT HCC [118]. Lin *et al*. evaluated the efficacy and toxicity of ^{125}I brachytherapy after transcatheter arterial chemoembolization in 77 patients with HCC complicated by PVTT [119]. The study showed that ^{125}I brachytherapy had a good therapeutic effect on these patients. Other studies also found that ISI combined with TACE significantly prolongs the median survival time of PVTT patients with liver cancer, improving the survival rate at 6, 12 and 18 months [120]. All evidence reveals that ISI combined with TACE is a safe and effective treatment for liver cancer tumor thrombosis [121].

^{125}I-seeds are low-energy radionuclides that provide long-term local control and improve survival in patients with HCC. Studies have shown that TACE combined with ^{125}I implantation is superior to TACE alone in the treatment of HCC [122]. By comparing the efficacy of TACE combined with ^{125}I seed implantation (TACE-^{125}I) and TACE combined with radiofrequency ablation (RFA) in the treatment of early and intermediate HCC, researchers believe that TACE combined with ISI may be an effective and safe alternative therapy for early and middle-stage HCC patients who cannot receive radiofold ablation or surgical treatment [123].

^{125}I brachytherapy can achieve a high local control rate in solid cancer. At the same time, the efficacy and safety of RFA in patients with local recurrence or residual HCC can prolong the progression-free survival of patients [102]. The efficacy of ISI was also demonstrated in the treatment of locally residual tumors in subphrenic HCC after TACE [124]. Tumor recurrence is a major problem after radical resection of HCC. Studies show that ^{125}I assisted brachytherapy significantly prolongs TTR and increases the OS rate after radical HCC resection [125]. ^{125}I combined with TACE also has good efficacy in the treatment of unresectable HCC complicated by obstructive jaundice [126]. Another CT-guided ^{125}I brachytherapy is safe and effective for bilateral lung recurrence after HCC resection or ablation [127].

In an investigation of seed-implantation methods, 1.5-T MRI-guided radiofrequency ablation combined with ISI was found to be an effective technique to treat HCC near great vessels [128]. In a single-center retrospective analysis, ISI guided by CT was evaluated as highly effective and safe in the treatment of challenging site lesions following TACE for HCC or CCC [129]. Even without the guidance of any imaging equipment, radioactive particles can be safely and effectively implanted into the tumor. Some scholars have discussed the anti-tumor mechanism of ^{125}I on HCC. They examined the effects of ^{125}I irradiation on glycolysis in HCCLM3 and SMMC-7721 cells. It was found that ^{125}I irradiation upregulates the inhibitory effect of miR-338 on phosphofructokinase of liver (PFKL) and down-regulates the Warburg effect of HCC. Thus, this approach could provide a new potential strategy for clinical treatment of HCC [130].

ISI and cytokine-induced killer cell therapy have been shown to be effective in the treatment of HCC. It is found that mice treated with a combination of radiation and immunotherapy had a significant reduction in tumor growth [131]. It is believed that ISI can up-regulate the expression of major histocompatibility complex I (MHC I) chain-associated gene A in HCC cells and enhance cytokine-induced killer cell-mediated apoptosis by activating caspase-3. In addition, cytokine-induced killer cells provide immune substrates that induce a strong immune response after ISI therapy. Therefore, ISI combined with cytokine-induced killer cell therapy can significantly inhibit the growth of human HCC cells *in vivo*, as well as improve the survival time of animals. This occurs through mutual promotion of anti-tumor immunity, which is a promising method for HCC treatment.

3.5. ^{177}Lu, ^{153}Sm, and ^{188}Re

^{177}Lu decays to stable hafnium (Hf 177) with a half-life of 6.65 d, emitting the most energetic beta radiation at 0.498 MeV and photon gamma radiation at 0.208 MeV and 0.113 MeV. The potential application value of [^{177}Lu]Lu-diethyltriamine pentaacetic acid-deoxyglucose (^{177}Lu-DTPA-DG) as a radiotherapy agent for liver tumor has been discussed [132]. Biodistribution, imaging, and radiotherapy of ^{177}Lu-DTPA-DG were studied using an SMMC-7721 model. The results showed that after ^{177}Lu-DTPA-DG radiotherapy, tumor growth was reduced, and overall survival was longer than that of the control group. Therefore, ^{177}Lu-DTPA-DG has the potential to be used as a hepatic radiopharmaceutical and is worthy of further study.

^{153}Sm has therapeutic advantages because of the emitting of therapeutic and diagnostic gamma radiation, in contrast to the simple β emitter ^{90}Y. Wong *et al*. developed neutron-activated [^{153}Sm]Sm carbonate (^{153}SmC)-labeled microspheres as an alternative to ^{90}Y-labeled hepatic radioembolism [133]. In the case of ^{153}SmC-labeled microspheres, the retention efficiencies of ^{153}SmC in distilled water and brine were 99% and 97%, which are higher than those of ^{153}Sm-labeled microspheres (~95% and ~85%, respectively). The characterization data showed that ^{153}SmC-labeled microspheres have good prospects for application in the treatment of hepatic radioembolism. However, this study lacked further studies on the safety and efficacy of application *in vivo*.

^{188}Re is an ideal therapeutic radionuclide with a half-life of 16.7 h. It can emit γ rays with maximum energy of 795 KeV, and the energy is moderate. The irradiation range within the tissue is short, which induces little damage to the tissue around the tumor. It also emits β rays simultaneously, which can be used for imaging. The main advantages are that the radionuclides do not need reactor production and can be easily obtained by a generator. Compared with other radionuclides, the cost is also lower, and inconve-

nience caused by transportation and storage can be avoided, which can help to reduce the treatment cost for liver cancer patients, facilitating the development of radionuclides for cancer treatment.

Because [^{188}Re]Re-LUF releases small ray energy with short half-life, the patient only needs to be hospitalized for 48 h after treatment without special protection after discharge, which leads to good compliance from patients. Good safety and tolerability with less adverse reactions with doses of up to 7400 MBq of [^{188}Re]Re-LUF intracoradiotherapy were appeared in one study examined 16 cases who could not be cured by surgery [134]. ^{188}Re-labeled microsphere (^{188}Re-MS) is another form of ^{188}Re for therapying HCC. Vega *et al*. developed a uniform-size and biodegradable ^{188}Re-MSs utilizing polylactic acid as a new and easy-to-image TARE reagent [135]. Microspheres were labeled with ^{188}Re and injected through an intrahepatic arterial catheter. Results indicated that ^{188}Re-MSs have potential as a new generation of TARE reagents. Future work should be done to investigate the therapeutic potential of ^{188}Re-MSs in large, long-term, preclinical studies and to evaluate the clinical outcomes of using ^{188}Re-MSs in different sizes.

3.6. ^{227}Th and ^{225}Ac

TAT is an emerging cancer targeted therapy strategy that utilizes specifically targeted delivery of alpha particles emitting radionuclides, such as ^{227}Th and ^{225}Ac, which can effectively kill cancer cells and limit bystander cytotoxicity in the tumor areas. Park's team reported the development of a ^{227}Th-labeled GPC3-targeted antibody conjugate ([^{227}Th]Th-octapa-αGPC3) for HCC treatment in an orthotopic mouse model, demonstrating highly specific targeting of GPC3 and significant tumor subduction in HepG2 tumor-bearing mice without acute off-target toxicity or animal death was observed [136]. In another study, Bell *et al*. synthesized [^{225}Ac]Ac-Macropa-GC33 using GC33, a full-length humanized monoclonal IgG1 specific to GPC, an 18-member heterocyclic crown ether. While, significant toxicity was observed, modest survival advantage was embodied, and a significant and rapid decrease in white blood cells was showed in hematological analysis in all radiation-coupled groups. Their study highlighted a significant disadvantage of TAT with directly labeled biomolecules with longer circulation times. The dose fractionation, pretargeting, and the use of smaller targeted ligands maybe reasonable strategies to mitigate the toxicity of TAT [137].

3.7. Induction and summary

Different radionuclides have different application stages and treatment methods in the treatment of HCC, and their main application characteristics are summarized in Table 2.

4. Discussion and outlook

HCC is a kind of cancer with complex and diverse etiology. For imaging diagnosis in this context, different methods are needed to obtain image information at different stages. Nuclear medicine can play an irreplaceable role in the early diagnosis, metabolism, blood supply, and metastasis of liver cancer; preoperative surgical planning and dose estimation; postoperative metastasis; recurrence; prognosis prediction; and other aspects. It could also provide important information for clinical diagnosis of liver cancer.

Clinical studies have shown that the sensitivity of [^{11}C]choline/[^{18}F]F-choline to detect HCC is higher than that of ^{18}F-FDG, especially for well-differentiated HCC. However, choline imaging agents can also be ingested by poorly differentiated HCC lesions, so it is impossible to evaluate the degree of differentiation solely based on the uptake of imaging agents. The combination of

Table 2
Major radionuclides used for radiotherapy of HCC.

Radionuclide	Half-life	Imaging type	Medicine	Application	Comment/Properties
^{90}Y	64.053 h	BS SPECT/PET	^{90}Y-microspheres: resin and glass	TARE	Combination of embolization and radiation therapy; safe, effective but expensive
^{166}Ho	26.824 h	SPECT/MRI	^{166}Ho- microspheres	TARE	Safe, effective and promising multimodal imaging
^{131}I	8.0252 d	SPECT	^{131}I-LUF	TARE	Cheap and readily available; effective; adjuvant therapy; postoperative patients need special protection because of long half-life
			^{131}I-mab	RIT	Effective; but there is a risk of missing the target
			^{131}I-nanoparticle	SIRT	Basic research stage and difficult to clinical transformation
^{125}I	59.407 d	PET	^{125}I-seed	SIRT	An alternative therapy for PVTT HCC
^{177}Lu	6.647 d	SPECT	[^{177}Lu]Lu-DTPA-DG	SIRT	Basic research stage
^{153}Sm	46.284 h	SPECT	^{153}SmC-microspheres	TARE	Lacked further studies on the safety and efficacy of application *in vivo*
^{188}Re	17.003 h	SPECT	[^{188}Re]*Re*-LUF	TARE	Special protection is not needed after discharge; few clinical studies
^{227}Th	18.68 d	/	[^{227}Th]Th-octapa -α*GPC3*	TAT	The new treatment strategy needs more *in vivo* studies to verify safety and effectiveness
^{225}Ac	10.0 d	/	[^{225}Ac]Ac-Macropa-GC33	TAT	

[^{11}C]choline/[^{18}F]F-choline can significantly improve the diagnostic value of HCC detection. In recent years, [^{68}Ga]Ga-PSMA-11 PET/CT has also been found to play an important role in the imaging diagnosis of HCC. Therefore, a larger series of studies is needed to better determine the clinical impact of the two-tracer PET model on HCC patients while taking dosiological considerations into account.

Although many PET or SPECT imaging probes are used in the diagnosis of HCC, there are still shortcomings in the early diagnosis, preoperative planning, and efficacy evaluation of liver cancer. To fully exploit the advantages of nuclear medicine and solve the major problems in HCC diagnosis, the need for specific probes with appropriate radionuclides will always be a research direction worth exploring. In order to improve the application of nuclear medicine in early diagnosis, cancer staging, preoperative planning, and prognosis evaluation of HCC, the research and development of imaging probes with more practical value will be of great significance for the diagnosis and monitoring of HCC by comprehensively considering rationality, science, and economy. Of course, limitations on the application of nuclear medicine in HCC also include the research, development, and application of imaging equipment. Furthermore, portable, multifunctional, integrated imaging equipment may be a future direction to explore.

HCC is considered to be radio-resistant [138], but the clinical value of radionuclide-based radiotherapy for HCC cannot be ignored. The effect of a single therapy on the treatment of HCC is often limited. In the fight against this kind of malignant tumor, it is often necessary to adopt a combination of two or more therapeutic measures according to the physical condition of the patient, tumor differentiation, blood supply, and immune environment of the tumor. For example, the combination of internal radiotherapy and chemotherapy drugs may improve the sensitivity of tumor cells to chemotherapy drugs or irradiation, as well as reduce the irradiation burden for patients. When combined with immunotherapy, radiotherapy can regulate the immune environment of the tumor and improve the effect of immunotherapy.

With the development of production technology and labeling methods, the application of radionuclides in the medical field will have more and more advantages. For the application of radionuclides in HCC, it is most important to solve the stability and targeting issues of radionuclides *in vivo*, to reduce the unnecessary irradiation of radionuclides to normal tissues, and to improve the accuracy of tumor diagnosis and the effectiveness of treatment. It is believed that the development of radionuclides will make significant contributions to the treatment of HCC.

Declaration of competing interest

The authors declare no conflict of interest.

Acknowledgments

This work was supported by the Major State Basic Research Development Program of China (No. 2017YFA0205201), and the National Natural Science Foundation of China (NSFC, Nos. 81925019 and U1705281).

References

[1] J.K. Stauffer, A.J. Scarzello, Q. Jiang, R.H. Wiltrout, Hepatology 56 (2012) 1567–1574.
[2] L.R. Roberts, C.B. Sirlin, F. Zaiem, Hepatology 67 (2018) 401–421.
[3] G. Gunasekaran, Y. Bekki, V. Lourdusamy, M. Schwartz, Hepatology 73 (2021) 128–136.
[4] C. Akateh, S.M. Black, L. Conteh, World J. Gastroenterol. 25 (2019) 3704–3721.
[5] A.K. Tong, W.Y. Tham, C.W. Too, Semin. Nucl. Med. 50 (2020) 419–433.
[6] L. Filippi, O. Schillaci, O. Bagni, Expert Rev. Med. Devices 16 (2019) 341–350.
[7] H. Ahmadzadehfar, H. Duan, A.R. Haug, S. Walrand, M. Hoffmann, Eur. J. Nucl. Med. Mol. Imaging 41 (2014) S115–S124.
[8] R. Cao, H. Liu, Z. Cheng, Curr. Med. Chem. 27 (2020) 6968–6986.
[9] M. Lee, H. Ko, M. Yun, Yonsei Med. J. 59 (2018) 1143–1149.
[10] P.R. Galle, F. Tovoli, F. Foerster, et al., J. Hepatol. 67 (2017) 173–183.
[11] P. d'Abadie, M. Hesse, A. Louppe, et al., Molecules 26 (2021) 3966.
[12] O. Öcal, D. Rössler, J. Ricke, M. Seidensticker, Dig. Dis. 10 (2021), doi:10.1159/000518101.
[13] M.M. Alauddin, Am. J. Nucl. Med. Mol. Imaging 2 (2012) 55–76.
[14] K. Mitamura, Y. Yamamoto, K. Tanaka, et al., Asia Ocean J. Nucl. Med. Biol. 3 (2015) 58–60.
[15] M. Tsurusaki, M. Okada, H. Kuroda, et al., J. Gastroenterol. 49 (2014) 46–56.
[16] L.J. Jr Wudel, D. Delbeke, D. Morris, et al., Am. Surg. 69 (2003) 117–126.
[17] A.R. Haug, Q. J. Nucl. Med. Mol. Imaging 61 (2017) 292–300.
[18] S. Wang, B. Li, P. Li, et al., Jpn. J. Radiol. 39 (2021) 1086–1096.
[19] E. Kong, K.A. Chun, I.H. Cho, PLoS One 12 (2017) e0180184.
[20] C.Y. Lin, J.H. Chen, J.A. Liang, et al., Eur. J. Radiol. 1 (2012) 2417–2422.
[21] E. Cho, C.H. Jun, B.S. Kim, et al., Turk. J. Gastroenterol. 26 (2015) 344–350.
[22] D.W. Sun, L. An, F. Wei, et al., Abdom. Radiol. 41 (2016) 33–41.
[23] J.W. Lee, J.K. Oh, Y.A. Chung, et al., J. Nucl. Med. 57 (2016) 509–516.
[24] A. Cistaro, F. Saglio, S. Asaftei, et al., Radiol. Case Rep. 6 (2011) 882–890.
[25] J.D. Lee, M. Yun, J.M. Lee, et al., Eur. J. Nucl. Med. Mol. Imaging 31 (2004) 1621–1630.
[26] S. Itoh, T. Yoshizumi, Y. Kitamura, et al., Hepatol. Commun. 5 (2021) 1278–1289.
[27] H.B. Wu, Q.S. Wang, B.Y. Li, et al., Clin. Nucl. Med. 36 (2011) 1092–1097.
[28] M. Bieze, H.J. Klumpen, J. Verheij, et al., Hepatology 59 (2014) 996–1006.
[29] M.A. Castilla-Lievre, D. Franco, P. Gervais, et al., Eur. J. Nucl. Med. Mol. Imaging 43 (2016) 852–859.
[30] J.N. Talbot, L. Fartoux, S. Balogova, et al., J. Nucl. Med. 51 (2010) 1699–1706.
[31] L. Fartoux, S. Balogova, V. Nataf, et al., Nucl. Med. Commun. 33 (2012) 757–765.
[32] J. Horsager, K. Bak-Fredslund, L.P. Larsen, et al., EJNMMI Res. 6 (2016) 56.
[33] Y. Li, D. Zhang, Y. Shi, et al., Contrast Media Mol. Imaging 11 (2016) 262–271.
[34] R. Chakravarty, S. Chakraborty, A. Dash, Mol. Pharm. 13 (2016) 3601–3612.
[35] H. Zhang, H. Cai, X. Lu, O. Muzik, F. Peng, Acad. Radiol. 18 (2011) 1561–1568.
[36] S. Li, C.G. England, E.B. Ehlerding, et al., Am. J. Transl. Res. 11 (2019) 6007–6015.
[37] J.G. Sham, F.M. Kievit, J.R. Grierson, et al., J. Nucl. Med. 55 (2014) 799–804.
[38] J.G. Sham, F.M. Kievit, J.R. Grierson, et al., J. Nucl. Med. 55 (2014) 2032–2037.
[39] X. Yang, H. Liu, C.K. Sun, et al., Biomaterials 35 (2014) 6964–6971.
[40] A. Natarajan, H. Zhang, W. Ye, et al., Cancers 13 (2021) 3977 (Basel).
[41] K.P. Labadie, A.D. Ludwig, A.L. Lehnert, et al., Sci. Rep. 11 (2021) 3731.
[42] R. Hernandez, H. Sun, C.G. England, et al., Theranostics 6 (2016) 1918–1933.
[43] J.A. Carrasquillo, J.A. O'Donoghue, V. Beylergil, et al., EJNMMI Res. 8 (2018) 20.
[44] X. Shi, H. Xing, X. Yang, et al., Eur. J. Nucl. Med. Mol. Imaging 48 (2021) 1593–1603.
[45] Y. Tolkach, D. Goltz, A. Kremer, et al., Oncotarget 10 (2019) 4149–4160.
[46] M. Kesler, C. Levine, D. Hershkovitz, et al., J. Nucl. Med. 60 (2019) 185–191.
[47] P. Mapelli, E. Incerti, F. Ceci, et al., J. Nucl. Med. 57 (2016) 43S–48S.
[48] Y.H. Kao, E.H. Tan, T.K. Teo, C.E. Ng, S.W. Goh, Ann. Nucl. Med. 25 (2011) 669–676.
[49] M. Wondergem, M.L. Smits, M. Elschot, et al., J. Nucl. Med. 54 (2013) 1294–1301.
[50] H. Ilhan, A. Goritschan, P. Paprottka, et al., J. Nucl. Med. 56 (2015) 1654–1660.
[51] J.J. Bailey, Y. Dewaraja, D. Hubers, R.N. Srinivasa, K.A. Frey, Clin. Transl. Imaging 5 (2017) 473–485.
[52] P. Haste, M. Tann, S. Persohn, et al., J. Vasc. Interv. Radiol. 28 (2017) 722–730.e1.
[53] M.G. Lam, M.L. Goris, A.H. Iagaru, et al., J. Nucl. Med. 54 (2013) 2055–2061.
[54] M. Yoshida, T. Beppu, S. Shiraishi, et al., Anticancer Res. 38 (2018) 3089–3095.
[55] M. Yoshida, S. Shiraishi, F. Sakamoto, et al., Ann. Nucl. Med. 28 (2014) 780–788.
[56] Y. Kai, R. Toya, T. Saito, et al., *In Vivo* 34 (2020) 3583–3588.
[57] B. Zhou, R. Wang, F. Chen, et al., ACS. Appl. Mater. Interfaces 10 (2018) 6146–6154.
[58] P.P. Hao, Y.P. Liu, C.Y. Yang, et al., PLoS One 9 (2014) e85002.
[59] C. Yang, Q. Yun, H. Sun, et al., Oncol. Lett. 7 (2014) 1919–1924.
[60] Y.S. Jhanwar, C. Divgi, J. Nucl. Med. 46 (2005) 141S–150S.
[61] R.M. Sharkey, D.M. Goldenberg, J. Nucl. Med. 46 (2005) 115S-127S.
[62] D.M. Goldenberg, R.M. Sharkey, Q. J. Nucl. Med. Imaging 50 (2006) 248–264.
[63] E.J. Lee, H.W. Chung, J.H. Jo, Y. So, Nucl. Med. Mol. Imaging 53 (2019) 367–373.
[64] M. Lyczko, M. Pruszynski, A. Majkowska-Pilip, et al., Nucl. Med. Biol. 53 (2017) 1–8.
[65] C. Parker, V. Lewington, N. Shore, et al., JAMA Oncol. 4 (2018) 1765–1772.
[66] B. Lambert, Eur. J. Nucl. Med. Mol. Imaging 32 (2005) 980–989.
[67] J.K. Mikell, Y.K. Dewaraja, D. Owen, Semin. Radiat. Oncol. 30 (2020) 68–76.
[68] A. Taebi, C.T. Vu, E. Roncali, J. Biomech. Eng. 143 (2021) 011002.
[69] J.C. Spina, I. Hume, A. Pelaez, et al., Radiographics 39 (2019) 578–595.
[70] K.T. Chan, A.M. Alessio, G.E. Johnson, et al., Int. J. Radiat. Oncol. Biol. Phys. 101 (2018) 358–365.
[71] M. D'Arienzo, M. Pimpinella, M. Capogni, et al., EJNMMI Res. 7 (2017) 94.
[72] L. Auditore, E. Amato, S. Boughdad, et al., Phys. Med. Biol. 65 (2020) 235014.
[73] M.F. Georgiou, R.A. Kuker, M.T. Studenski, et al., EJNMMI Res. 11 (2021) 96.
[74] A. Ezponda, M. Rodríguez-Fraile, M. Morales, et al., Cardiovasc. Interv. Radiol. 43 (2020) 987–995.
[75] F.E. Boas, L. Bodei, C.T. Sofocleous, J. Nucl. Med. 58 (2017) 104S–111S.

[76] I. Kurilova, A. Bendet, E.K. Fung, et al., Abdom. Radiol. 46 (2021) 3428–3436 (NY).
[77] M. Zimmermann, M. Schulze-Hagen, F. Pedersoli, et al., World J. Radiol. 11 (2019) 102–109.
[78] A.C. Gordon, S.B. White, V.L. Gates, et al., Acad. Radiol. 28 (2021) 849–858.
[79] A.C. Gordon, S.B. White, Y. Yang, et al., Cardiovasc. Interv. Radiol. 43 (2020) 1528–1537.
[80] N.J.M. Klaassen, M.J. Arntz, A.A. Gil, et al., EJNMMI Radiopharm. Chem. 4 (2019) 19.
[81] A.J.A.T. Braat, J.F. Prince, R. van Rooi, et al., Eur. Radiol. 28 (2018) 920–928.
[82] J. Roosen, M.J. Arntz, M.J.R. Janssen, et al., Cancers 13 (2021) 5462 (Basel).
[83] M.L.J. Smits, M.G. Dassen, J.F. Prince, et al., Eur. J. Nucl. Med. Mol. Imaging 47 (2020) 798–806.
[84] M. Elschot, J.F. Nijsen, M.G. Lam, et al., Eur. J. Nucl. Med. Mol. Imaging 41 (2014) 1965–1975.
[85] C. Chiesa, M. Maccauro, Eur. J. Nucl. Med. Mol. Imaging 47 (2020) 744–747.
[86] J.F. Prince, R.V. Rooij, G.H. Bol, et al., J. Nucl. Med. 56 (2015) 817–823.
[87] M. Stella, A.J.A.T. Braat, M.G.E.H. Lam, et al., EJNMMI Phys. 8 (2021) 22.
[88] R. van Rooij, A.J.A.T. Braat, H.W.A.M. de Jong, et al., EJNMMI Phys. 7 (2020) 13.
[89] J.F. Prince, M.A.A.J. van den Bosch, J.F.W. Nijsen, et al., J. Nucl. Med. 59 (2018) 582–588.
[90] R. Bastiaannet, C. van Roekel, M.L.J. Smits, et al., J. Nucl. Med. 61 (2020) 608–612.
[91] K. Yavari, E. Yeganeh, H. Abolghasemi, J. Label. Compd. Radiopharm. 59 (2016) 24–29.
[92] S. Subramanian, K.V. Vimalnath, A. Dash, J. Label. Comp. Radiopharm. 61 (2018) 509–514.
[93] W.Y. Lau, T.W.T. Leung, S.K.W. Ho, et al., Lancet 353 (1999) 797–801.
[94] J.L. Raoul, P. Bourguet, J.F. Bretagne, et al., Radiology 168 (1988) 541–545.
[95] L. Schwarz, M. Bubenheim, I. Gardin, et al., World J. Surg. 40 (2016) 1941–1950.
[96] R. Furtado, M. Crawford, C. Sandroussi, Ann. Surg. Oncol. 21 (2014) 2700–2707.
[97] J.L. Chi, C.C. Li, C.Q. Xia, et al., Radiat. Res. 181 (2014) 416–424.
[98] Y. Qian, Q. Liu, P. Li, et al., ACS Nano 15 (2021) 2933–2946.
[99] F. Pang, Y. Li, W. Zhang, et al., Adv. Healthc. Mater. 9 (2020) e2000028.
[100] J. Xu, H.Y. Xu, Q. Zhang, et al., Mol. Cancer Res. 5 (2007) 605–614.
[101] H. Niu, R. Wang, J. Cheng, S. Gao, B. Liu, Oncol. Rep. 30 (2013) 246–252.
[102] L. Wu, B. Sun, X. Lin, et al., Genes Cells 23 (2018) 35–45.
[103] B. Lambert, C. Van de Wiele, Eur. J. Nucl. Med. Mol. Imaging 32 (2005) 980–989.
[104] A.I. Kassis, S.J. Adelstein, J. Nucl. Med. 46 (2005) 4S–12S.
[105] Z.N. Chen, L. Mi, J. Xu, et al., Int. J. Radiat. Oncol. Biol. Phys. 65 (2006) 435–444.
[106] Q. Zhang, J. Zhou, X.M. Ku, et al., Eur. J. Cancer Prev. 16 (2007) 196–202.
[107] H. Bian, J.S. Zheng, G. Nan, et al., J. Natl. Cancer Inst. 106 (2014) u239.
[108] J. Xu, Z.Y. Shen, X.G. Chen, et al., Hepatology 45 (2007) 269–276.
[109] W. Fan, Y. Wu, M. Lu, et al., Clin. Res. Hepatol. Gastroenterol. 43 (2019) 451–459.
[110] Q. He, W.S. Lu, Y. Liu, Y.S. Guan, A.R. Kuang, World J. Gastroenterol. 19 (2013) 9104–9110.
[111] A. Vogel, A. Saborowski, Lancet Gastroenterol. Hepatol. 5 (2020) 517–519.
[112] H. Chen, H.W. Cheng, W.Y. Wu, et al., Chin. Chem. Lett. 31 (2020) 1375–1381.
[113] M. Lin, Y. Xiao, X. Jiang, et al., J. Nanomater. 2020 (2020) 1–15.
[114] M. Lin, J. Huang, D. Zhang, et al., Anal. Cell. Pathol. 2016 (2016) 9142198 (Amst).
[115] A. Ji, Y. Zhang, G. Lv, et al., J. Label. Comp. Radiopharm. 61 (2018) 362–369.
[116] M. Yang, Z. Fang, Z. Yan, et al., J. Cancer. Res. Clin. Oncol. 140 (2014) 211.
[117] S. Li, J.H. Guo, J. Lu, et al., Cancer Radiother. 25 (2021) 340–349.
[118] J. Lin, H. Jiang, W. Yang, et al., Brachytherapy 18 (2018) 233–239.
[119] H. Sun, M. Zhang, R. Liu, et al., Future Oncol. 14 (2018) 1165–1176.
[120] D. Yuan, Z. Gao, J. Zhao, H. Zhang, J. Wang, Brachytherapy 18 (2019) 521–529.
[121] W. Wang, C. Wang, J. Shen, et al., Cardiovasc. Intervent. Radiol. 44 (2021) 1570–1578.
[122] Z.X. Zhu, X.X. Wang, K.F. Yuan, J.W. Huang, Y. Zeng, HPB 20 (2018) 795–802.
[123] L. Chen, X. Kan, T. Sun, et al., BMC Gastroenterol. 20 (2020) 205.
[124] J. Li, L. Zhang, Q. Xie, et al., Brachytherapy 18 (2019) 420–425.
[125] K. Chen, Y. Xia, H. Wang, et al., PLoS One 8 (2013) e57397.
[126] S. Li, X. He, L. Dang, et al., Dig. Dis. Sci. 63 (2018) 321–328.
[127] Z. Xiang, M. Bai, G. Li, et al., J. Cancer Res. Clin. Oncol. 145 (2019) 1907–1916.
[128] Z.Y. Lin, J. Chen, X.F. Deng, Eur. J. Radiol. 81 (2012) 3079–3083.
[129] J. Li, L. Zhang, Z. Sun, et al., J. Contemp. Brachyther. 12 (2020) 233–240.
[130] J. Zheng, J. Luo, H. Zeng, L. Guo, G. Shao, Biomed. Pharmacother. 119 (2019) 109402.
[131] J. Zhang, N. Wu, Z. Lian, et al., Technol. Cancer. Res. Treat. 16 (2017) 1083–1091.
[132] L. Zhou, L. Chen, L. Yang, et al., Cancer. Biother. Radiopharm. 35 (2020) 33–40.
[133] Y.H. Wong, H.Y. Tan, A. Kasbollah, B.J.J. Abdullah, C.H. Yeong, Pharmaceutics 11 (2019) 596.
[134] P. Bernal, J.L. Raoul, G. Vidmar, et al., Int. J. Radiat. Oncol. Biol. Phys. 69 (2007) 1448–1455.
[135] J.C. De La Vega, P.L. Esquinas, C. Rodríguez-Rodríguez, et al., Theranostics 9 (2019) 868–883.
[136] K.P. Labadie, D.K. Hamlin, A. Kenoyer, et al., J. Nucl. Med. (2021), doi:10.2967/jnumed.121.262562.
[137] M.M. Bell, N.T. Gutsche, A.P. King, et al., Molecules 26 (2020) 4.
[138] R. Gallicchio, A. Nardelli, P. Mainenti, et al., Biomed. Res. Int. 2016 (2016) 1295329.